TiO₂ From Colloidal Dispersion as Support in Pt/TiO₂ Nanocomposite for Electrochemical Applications†

Milica Košević,[1] Gavrilo Šekularac,[1] Ljiljana Živković,[2] Vladimir Panić,[1,*] Branislav Nikolić[3]

[1] Institute of Chemistry, Technology and Metallurgy, University of Belgrade, Njegoševa 12, RS-11000 Belgrade, Serbia

[2] Vinča Institute of Nuclear Sciences, University of Belgrade, Mike Petrovića Alasa 12-14, RS-11001 Belgrade, Serbia

[3] Faculty of Technology and Metallurgy, University of Belgrade, Karnegijeva 4, RS-11000 Belgrade, Serbia

* Corresponding author's e-mail address: panic@ihtm.bg.ac.rs

─── THIS PAPER IS DEDICATED TO PROF. MIRJANA METIKOŠ-HUKOVIĆ ON THE OCCASION OF HER BIRTHDAY ───

Abstract: TiO₂ powder was synthesized by a forced hydrolysis process and used for the synthesis of Pt/TiO₂ composite that is to be foreseen as an advanced electrode material. Pt was incorporated into the synthesized TiO₂ from a Pt colloidal dispersion as a precursor prepared by a microwave-assisted polyol process. Physicochemical properties of TiO₂ and TiO₂-supported Pt were investigated by scanning electron microscopy, dynamic light scattering and X-ray spectroscopy and diffraction techniques. The properties of Pt/TiO₂ composite are correlated to the basic voltammetric response of its thin-layer form. It was found that subsequent thermal treatment of synthesized TiO₂, which caused crystallization into mainly rutile phase, is required for appropriate Pt incorporation. Although being appropriately loaded by Pt, and the voltammetric response is typical for Pt-based material, the voltammetry of Pt/TiO₂ corresponded to much lower loadings. The possibility for Pt particles to be trapped inside TiO₂ agglomerates is indicated. The catalyst usage from the synthesized Pt/TiO₂ was found quite moderate due to this trapping.

Keywords: titania, platinum as electrocatalyst, particle size distribution, hydrothermal synthesis, catalyst support.

INTRODUCTION

TITANIUM OXIDE in catalysis is mostly known upon its photocatalytic and photoelectrocatalytic activity, especially in heterogeneous catalysis of organic compounds.[1,2] Although being considered generally as an n-type semiconductor[3], titania also found the application in electrocatalysis as a stabilizing component of the electroactive coatings of activated titanium anodes[4] and potentially interactive support for nanoparticular metallic electrocatalysts, *e.g.*, Pt.[5] Rutile and anatase are the two most common crystal forms (polymorphs) of TiO₂. Although anatase has a higher photocatalytic activity than rutile, rutile has certain advantages over anatase: it is more stable and has a narrower band gap.[6] It is known that energy band gap has a great impact on the catalytic activity of semi-conductive materials, which implies that the analysis of the anatase–rutile relationship should be one of the most important properties of synthesized TiO₂ and Pt/TiO₂ as advance catalytic materials. In addition, but most important for the bifunctional electrocatalysis, Pt/TiO₂ combination fits well to interactive interionic bonding theory[7] for the hyper-d metallic electrocatalysts supported on hypo-d oxide.

In last decades, fuel cell (FC) investigations are continuously expanding, due to the increasing demands for sustainable energy production and consumption.[8–10] Current research activities are directed toward FC reliability and durability.[11,12] The durability of a proton exchange membrane (PEM) FCs is highly dependent on the stability of the electrocatalyst; thus, selection of the proper electrode material in an FC is very important.[13] Platinum nanoparticles deposited onto powdered carbon substrates are widely used electrocatalysts in FCs.[6,14,15] Carbon as electrocatalyst support has disadvantages, mainly due to low stability and low resistivity to corrosion.[4,16,17] These

† Dedicated to dear Prof. Mirjana Metikoš-Huković for valuable contribution to electrochemical science on the occasion of her jubilee birthday

disadvantages cause the loss of the electrochemically active surface area.[18–20] Hence, the development of alternative catalyst carriers to carbon is attracting increasing attention. TiO_2 appears to be suitable replacement since it is at least of low cost and high stability.[21–23] The synthesis of Pt/TiO_2 needs to be carefully tailored to meet the demands for promising electrocatalytic materials of the next generation, especially for the cathodic FC reactions.[4] It was found that TiO_2 enhances the Pt activity for oxygen reduction reaction[24], which is assigned to increased electron density on Pt due to partial charge transfer from oxide to metal nanoparticles.[25]

It follows that controlled synthesis of the TiO_2 support, leading to finely dispersed particles of defined size, shape and structure, could be a valuable effort towards advances in electrocatalysis. Since the process of forced hydrolysis is seen as a promising procedure for simple and well described synthesis of TiO_2,[26] it was applied in this work as the basis for the preparation of the TiO_2 support for Pt nanoparticles.

In a previous work, a preliminary estimation of the voltammetric response and stability of Pt/TiO_2 composite was briefly reported.[27] It was found that the activity decreased upon cycling, which was more pronounced at lower sweep rates. This finding was assigned to less reversible Pt particles transformations at lower sweep rates, including agglomeration and coarsening, as the most probable cause.

This paper investigates in details the structural causes for the registered cycling voltammetry of the oxide/metallic particles. The subjects are *ex-situ* synthesized TiO_2 powders, obtained by forced hydrolysis of Ti chloride, which were combined with the solvatothermally-prepared Pt colloidal dispersion to obtain the composite by the traditional polyol procedure.[28] The synthesized oxide structures and/or composites were examined by microscopic and spectroscopic methods and techniques related to light scattering and X-ray diffraction. The aim was to gain knowledge for the assessment of the conditions for synthesis of catalytically prominent metal/oxide composites.

EXPERIMENTAL

TiO₂ Synthesis

This synthesis procedure followed the forced hydrolysis process, already applied for the synthesis of TiO_2.[21,29] Briefly, $TiCl_3$ was added drop wise into a boiling 0.7 mol dm^{-3} HCl solution, to obtain the $TiCl_3$ solution of 21.5 g dm^{-3}. During 90 min boiling under reflux, a part of the TiO_2 particles, generated in the reaction mixture, aggregated in a loose precipitate. This solid was washed by water and dried (110 °C) to form TiO_2 powdered material. The powder was used for the preparation of Pt/TiO_2 catalyst, either as-synthesized (TiO_2nt), or thermally treated at 400 °C for 180

min in air (TiO_2tt). The stable part of the reaction mixture, *i.e.*, TiO_2 colloidal dispersion, was ultra-filtered upon dilution with water to pH 4.0, to increase the concentration of the dispersed phase for reliable further investigation. The ultra-filtration (UF) was performed in 200-mL Amicon® UF stirred cell under a N_2 pressure of 5 bar through 5 kDa Millipore Ultracel® UF membrane made of regenerated cellulose.

Pt Colloid Synthesis

Pt colloid was synthesized by the standard, microwave-assisted polyol process.[22] A chloroplatinic acid solution (8 wt. % in H_2O, Aldrich) in water, 0.01 mol dm^{-3}, was slowly added to the excess of ethane-1,2-diol, which served for the reduction of Pt^{4+} and as a stabilizing agent to produced Pt particles; the mixture was stirred for 15 min on a magnetic stirrer. 0.1 M NaOH was added drop-wise to increase the pH to 12. This mixture was placed in a microwave oven at 70 W for 1 min. Consequently, the initial yellow-colored and transparent medium turned into darkish, moderately transparent one, due to generation of Pt nanoparticles. This synthesis procedure was proved to generate small Pt particles, of a few nm in size, and with a narrow particle size distribution.[22]

The Synthesis of Pt/TiO₂ Composite

Pt was deposited onto as-synthesized or thermally treated TiO_2 powders as follows: 1 g dm^{-3} of TiO_2nt or TiO_2tt were ultrasonically dispersed in H_2O and added into 150 ml of 2 mol dm^{-3} H_2SO_4. The obtained suspension was stirred for 15 min and Pt dispersion was subsequently added. The stirring was continued for 180 min. Upon filtration and rinsing with water, the obtained Pt/TiO_2 composite was thermally treated at 160 °C under a N_2 atmosphere.

Material Characterization

The microscopic appearance of the TiO_2 powders and Pt/TiO_2 composite was investigated by scanning electron microscope (SEM) Jeol JSM 5800, operated at 20 keV. The loading of Pt deposited onto TiO_2 support was characterized by Energy dispersive spectroscopy (EDS), type Oxford Inca 3.2, coupled with SEM.

The particle size distribution of the TiO_2 precipitate, re-dispersed in water and water+ethane-1,2-diol (EG), in 6:1 volume ratio, and the UF-treated TiO_2 colloidal dispersion was analyzed by dynamic light scattering (DLS, Zetasizer Nano ZS instrument, Malvern Instruments Ltd., UK). The zeta potential of some of the samples was also measured by the same equipment. In order to follow the DLS response stability of the dispersions, several successive measurements were performed within each DLS measurement. The X-ray diffraction (XRD) pattern of TiO_2 powders was obtained on an Ultima IV Rigaku diffractometer, using

Croat. Chem. Acta **2017**, *90*(2), 251–258

DOI: 10.5562/cca3175

CuKα1,2 radiation, with a generator voltage and current of 40.0 kV and 40.0 mA, respectively. The 2θ range of 5–90 ° was used for the XRD analysis in the continuous scan mode with a scanning step size of 0.05 ° and at a scan rate of 5 °/min. Fourier-transform infrared (FTIR) spectra were recorded on Bomem (Hartmann & Braun, Germany) spectrometer in transmission mode between 400 and 4000 cm⁻¹ with a resolution of 4 cm⁻¹ using the standard KBr method.

It is to be mentioned that DLS, XRD and FTIR characterizations have not been performed for Pt colloidal dispersion and Pt/TiO₂ composite, since Pt is synthesized *ex-situ* by standard polyol procedure,[28] and corresponding structural properties are considered as known.

Cyclic Voltammetry Measurements

The composite suspension for the preparation of thin layer electrodes was formed by mixing 3 mg of Pt/TiO₂ powder and 50 µL of Nafion® solution (Aldrich, 5 wt. % in lower aliphatic alcohols and 15–20 % water) with 1 ml H₂O. The obtained suspension was stabilized ultrasonically (40 kHz, 70 W) for 60 min. The suspension was pipetted onto a glassy carbon (GC, Sigradur – Sigri, Elektrographite, GMbH, Germany) electrode (A = 0.196 cm²) and room-dried to form a thin 0.31 mg cm⁻² layer of composite. The cyclic voltammetric (CV) response in de-aerated 0.1 mol dm⁻³ HClO₄ was checked at the sweep rate of 50 mV s⁻¹ in a standard three-electrode cell configured with a Pt-mesh as the counter electrode and Ag/AgCl electrode (in saturated KCl, 0.197 V *vs*. SHE) as the reference. All potentials in up-and-coming sections are referred to the Ag/AgCl electrode.

RESULTS AND DISCUSSION

Particle Size Distribution (PSD) of the Synthesized TiO₂

In 90 min of the forced hydrolysis of TiCl₃, a white precipitate was continuously formed, which started already after *ca*. 30 min of boiling under reflux. Both the colloidal dispersion in equilibrium with the precipitate and the precipitate, dried and re-dispersed in water and water+EG, were subjected to PSD analysis by dynamic light scattering (DLS), Figure 1. PSD analysis aimed to correlate the characteristics of TiO₂ particles formed by forced hydrolysis to those subjected to Pt incorporation.

Two well-resolved particle fractions were registered in the colloidal dispersion (given by intensity (a1 and b1)
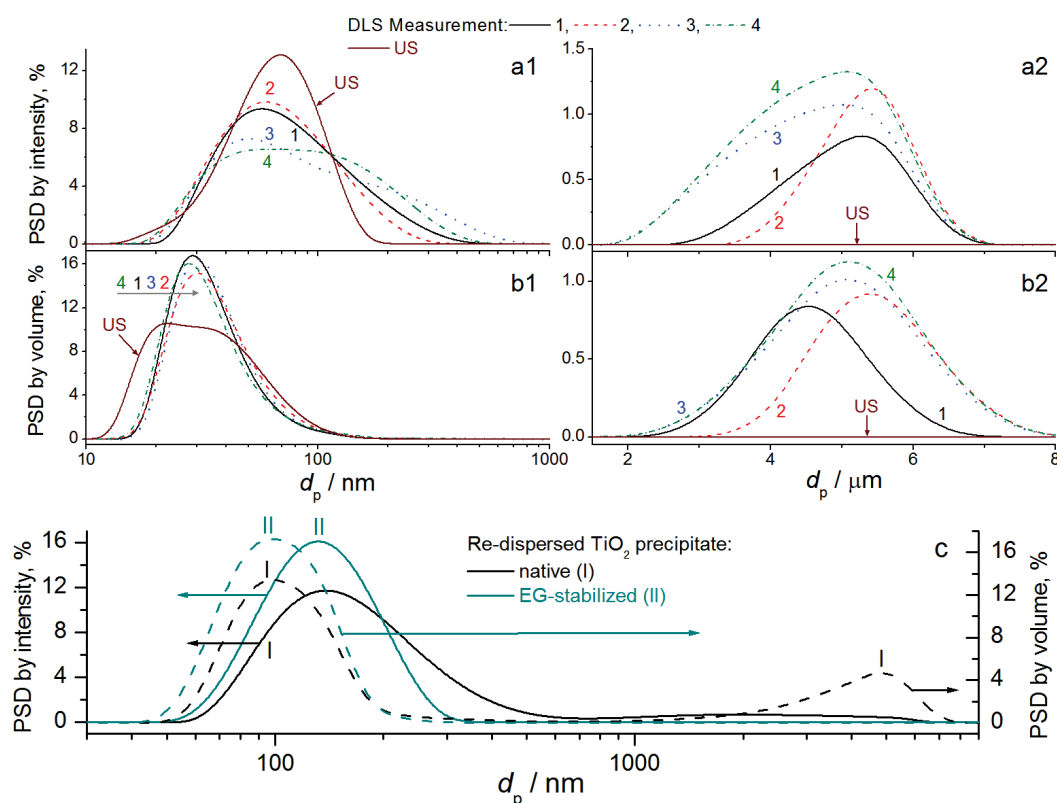
Figure 1. DLS-generated PSDs by intensity (a1 and a2) and volume (b1 and b2) of the TiO₂ colloidal dispersion during four successive measurements and after 1 min-ultra-sonication (US) with separated small (a1 and b1) and large (a2 and b2) particle size region; c) the TiO₂ precipitate re-dispersed in water, native and stabilized by ethane-1,2-diol (EG).

and volume (a2 and b2) distribution in Figure 1): one with the size ranging from 15 to 400 nm and the other of 2–7 µm-sized agglomerates of weakly-joined particles. This result shows that synthesized dispersion is highly polydisperse, due to high tendency of native particles to join into bigger ones able to form agglomerates. Both fraction peaks become wider in the PSD spectra of 4 successive DLS measurements, with a decrease in the intensity of the low-d_p fraction and corresponding increase for the agglomerate fraction (Figure 1, a1 and a2, respectively), which indicates high tendency of the particles to join and precipitate.[30] The first peak, initially located around 60 nm, evolves and finally resolves into two shoulders around 50 and 200 nm in last two DLS measurements (a1). The agglomerates had a stable d_p around 5 µm, but of increasing intensity of the scattered light (a2), which indicates that number of agglomerates continuously increases. This increase could be due to aggregation of the smaller particles, also registered as their increasing share in the PSD by volume (b2). In addition, the PSDs by volume clearly show that the low-d_p DLS response (b1) was dominated by particles of around 30 nm in size, *i.e.*, the most abundant particles in the dispersion. However, these particles appear not to be the native ones, since short ultra-sonication (1 min) resulted in the separation of the 30-nm volume peak into the peaks at 20 and 40 nm, which can be attributed to the native particles and their twins, respectively. No agglomerates were detected upon ultra-sonication. The result clearly indicates weak gathering force of the native particles in the agglomerates, although their presence originates from the instability of the dispersion and the formation of the precipitate.

The above-discussed stability issues were fairly reflected in the DLS response of the precipitate re-dispersed in water (Figure 1c). There was a peak of intensity at around 150 nm, which is quite close to the position of the mediate fraction appearing during continuous destabilization of the colloidal dispersion (1st to 4th DLS measurement, a1 and b1). In addition, the presence of agglomerates was clearly confirmed with an intensity fraction over a very wide d_p range, 700 nm-6 µm. However, the volume peak indicated the dominance of the 5 µm-sized agglomerates as in the case of the colloidal dispersion. The main difference between the DLS response of colloidal dispersion and re-dispersed precipitate was reflected in the difference between the positions of intensity and volume peaks in the low-d_p region. Namely, the volume peak for the re-dispersed precipitate was only slightly moved toward lower d_p value (100 nm), which indicates considerably less pronounced polydispersity of the re-dispersed precipitate in the region of lower d_p in comparison to colloidal dispersion.

Since the precipitate was of less pronounced polydispersity, it was foreseen for combination with the Pt colloidal dispersion to generate the Pt/TiO₂ catalyst. In addition,

the smallest registered fraction in colloidal dispersion (below 20 nm) as the main constituent of the dispersed phase, appears to small to act as a host for Pt particles of a few nm in size.[28]

Since EG acts as a stabilizing agent for the colloidal Pt particles, it was also found capable of suppressing the formation of large particles and agglomerates in the re-dispersed TiO₂ precipitate (EG-stabilized sample, Figure 1c). Indeed, the low-d_p PSD responses of EG-stabilized sample were better resolved than in the EG-free medium (native re-dispersion in Figure 1c) and slightly shifted toward lower d_p values. Moreover, particles with a diameter greater than 300 nm were not registered.

In addition to the advantageous PSD properties of the EG-stabilized TiO₂ re-dispersed phase for a preparation of Pt/TiO₂ composite, the surface charge of TiO₂ and Pt should be of different sign. The measured zeta potentials for the EG-stabilized TiO₂ and Pt colloidal dispersion were 31.2 and −26.9 mV, respectively. It follows that required physicochemical conditions were fulfilled for TiO₂ particles to accommodate Pt particles on their surface.

The Structure and Surface Appearance of the Synthesized Materials

XRD analysis shows that the synthesized oxide had a rather amorphous structure, with only weak indication of crystallization in the 2θ range 20–30 ° appearing at the position where typically the most intense reflections of rutile and anatase structures appear (Figure 2). Thermal treatment of the synthesized TiO₂ develops crystalline structure, with peaks typical for the reflections from the planes of rutile. The dominant peak, located at a 2θ value of 27.4 °, relates to (110) plane. The appearance of the anatase structure could also be noticed as a weak shoulder at the position of the most intense (101) anatase plane reflection around a 2θ value of 25 °. To estimate the TiO₂ crystallite size, the Scherrer equation was applied to the (110) peak parameters. The calculated size of the TiO₂ crystallites was 18 nm. This value agrees very well with the DLS findings related to the US-treated dispersion (Figure 1, b1), which clearly
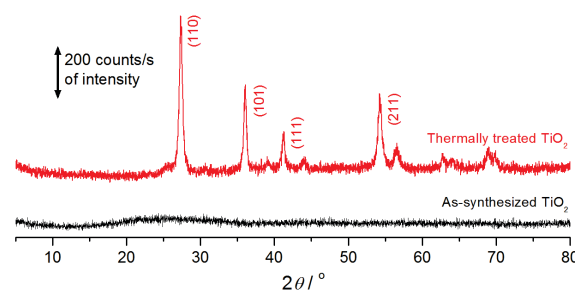
Figure 2. XRD patterns of the as-synthesized and thermally treated precipitate from the forced hydrolysis synthesis of TiO₂.

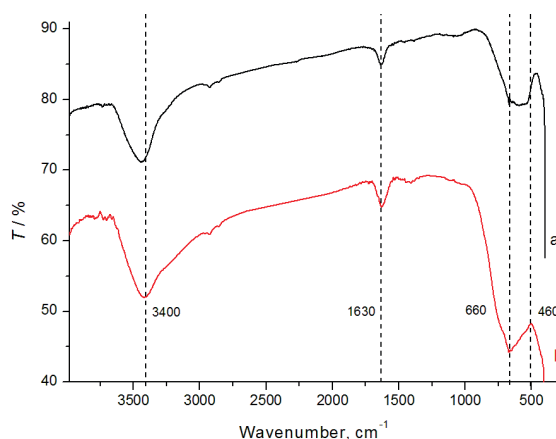**Table 1.** EDX results of the composition of Pt/TiO₂tt gained from Figure 5.

Position	Element content, at. %			Pt Content, wt. %
	Ti	Pt	O	
1	24.6	2.8	72.6	19.3
2	20.6	2.5	76.9	17.6
3	17.4	2.2	80.4	15.6
Average	20.9	2.5	76.6	17.5

indicated the smallest particles with the size of around 20 nm. Hence, it follows that TiO_2 solid phase actually consisted of particle clusters and agglomerates formed by elemental units of 20-nm-sized crystallites.

Since XRD indicated the presence of both rutile and anatase phase, the synthesized TiO_2 samples were subjected to FTIR analysis to check the differences in the metal–oxygen bond response between TiO_2nt and TiO_2tt. The registered spectra are shown in Figure 3.

Although the degrees of crystallinity of the investigated samples were found to be different by XRD, the FTIR spectra appear quite similar in the range of higher wavenumbers. There is a pronounced peak at around 3400 cm⁻¹ as the response of O–H bonds, and a smaller peak at around 1630 cm⁻¹ usually assigned to adsorbed water.[31,32]

The differences in spectra are seen in the wavenumber range of IR response of the Ti–O bonds, 400–1000 cm⁻¹. For the thermally treated sample of defined, mostly rutile structure, there is a well-resolved peak at 660 cm⁻¹, which is considered as typical for metal/oxygen bond of the rutile structure.[33] On the other hand, there is a broad IR adsorption in the 460–660 cm⁻¹ range for the as-synthesized sample, which presumably arose from amorphous material. The broad response in the mentioned

range of the FTIR spectrum appears to be characteristic of the anatase structure.[34,35] This shows that the almost XRD-amorphous structure, with only weak indication of crystalline domains, is in the state of the initially created mainly anatase structure.

The micro-appearance of the powders synthesized by forced hydrolysis is shown in Figure 4. The as-synthesized dried TiO_2 powder, obtained from the precipitate, dominantly consisted of particles with diameters below 500 nm, which are joined into weak agglomerates of several μm in size, appearing sporadically in Figure 4a. This is in good agreement with the DLS findings (Figure 1c).
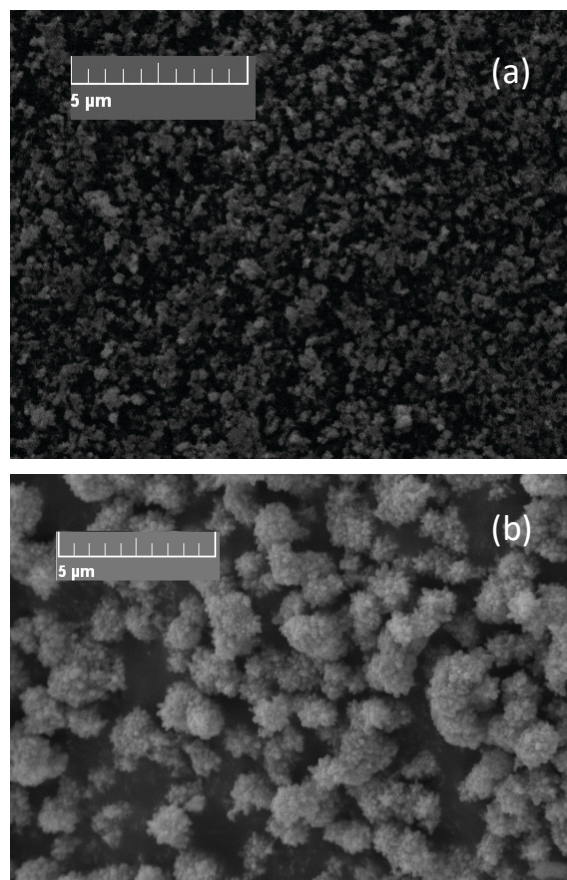

Figure 4. SEM images of the dried TiO_2 powders: a) as-synthesized; b) thermally treated at 400 °C.

Figure 3. FTIR spectra of the hydrothermally synthesized TiO_2: a) as-synthesized and dried, and b) subsequently thermally treated at 400 °C.

The thermal treatment induces the overall agglomeration of the well-defined spherical particles (Figure 4b). The particles constituting the agglomerates are also of diameters below 500 nm, similar to those from thermally non-treated TiO_2 powder (Figure 4a). The agglomerates appear compact and of well-defined shape, with a size distribution ranging from 1 to 3 μm.

SEM image of the TiO_2tt (Figure 4b) showed that the TiO_2 particles tended to form almost 2 μm-sized agglomerates of ellipsoidal shape (on average, the diameters were: $a = 1100$ nm, $b = c = 765$ nm).

The synthesized TiO_2 powders were used further for the synthesis of Pt/TiO_2 composite. For this purpose, the powders were dispersed in a mixture of sulfuric acid, water and EG and subsequently mixed with a Pt EG dispersion. The appearance of resulting Pt/TiO_2 composite was not considerably different from the native TiO_2tt; as an illustration, the SEM image of Pt/TiO_2tt is given in Figure 5. The sample contained large aggregates appearance similar to the TiO_2tt support. Although the stabilizing effect of EG (150 nm-sized particles) is seen in Figure 1c, it seems that a considerable decrease in pH during the preparation of the composite (addition of sulfuric acid into the Pt deposition mixture) induced particles re-agglomeration. If the sizes of agglomerates are compared, Figures 4b and 5, a small difference could be noticed, *i.e.*, Pt/TiO_2tt consisted of slightly larger agglomerates ($a = 1475$ nm, $b = c = 657$ nm). This indicated that Pt could be incorporated much more throughout the volume of agglomerates than on the surface of the TiO_2 particles. Consequently, this constitution affected the characteristic electrochemical response of the composite as discussed in next section. It should be noted that the electrochemical properties of Pt/TiO_2nt were found to be poor, and hence, this sample was not subjected to further characterization.

In order to analyze the composition of the Pt/TiO_2tt composite, EDX measurements were performed. The data obtained at three different positions, indicated in Figure 5, are presented in Table 1. The Pt content was found to be fairly close to 20 wt. %, as expected from the synthesis procedure. It was also quite similar to that determined spectrophotometrically in previous investigation (19 wt. %).[21] Table 1 shows that the oxygen content is higher with respect to that expected from the TiO_2. This could be explained by some Pt being present as oxide, but oxidation of Pt during the polyol synthesis procedure is unlikely. Rather, the excess of oxygen could reasonably be assigned to the presence of water, as indicated by FTIR (Figure 3). The data from Table 1 could then correspond to a water content between 2.5 and 3 mol per 1 mol of TiO_2, and the data for the Pt content also has to take into account the water content. This approach in calculation of Pt content could result in smaller values with respect to spectrophotometric/gravimetric
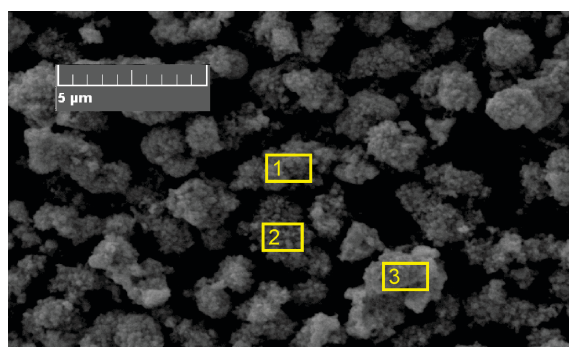
Figure 5. SEM image of Pt supported on thermally treated TiO_2; yellow rectangles indicate the positions at which EDX data (Table 1) were obtained.

methods and the pre-set value of 20 wt. %, which were based on TiO_2, and not on its possible hydrous form.

The analysis of the composite composition clearly showed that thermally treated TiO_2 is able to adopt *ex-situ* synthesized Pt particles.

Electrochemical Properties of Pt/TiO₂ from CV Response

Stable CV cycles[21] of synthesized Pt/TiO_2 are shown in Figure 6. An almost featureless voltammogram is registered for the composite with thermally non-treated TiO_2. Just an indication of the Pt oxide formation/reduction is seen around 0.5 V, whereas the hydrogen adsorption/desorption is even less pronounced. CV response of Pt was weak since conductivity of the material was low, due to certain amount of loosely distributed Pt particles onto generated oxide structure.

Thermal treatment of TiO_2 improved considerably the CV features of Pt. There are typical regions of oxide formation/reduction (above/below 0.6 V) and two well-developed peaks in hydrogen adsorption/desorption region. The influence of thermal treatment seems to be related to the development of defined TiO_2 crystalline structure as found by the XRD analysis. Although the CV of Pt/TiO_2tt is typical for nanostructured Pt in acid solution, the registered CV currents were considerably lower in comparison to Pt/C composite counterpart, as it was already found during a preliminary investigation of the CV response stability.[27]

The reported consideration indicate that only Pt from the surface of the agglomerates could contribute to the measured CV response (the loading of 7-nm-sized Pt particles[27] calculated from CV of Pt/TiO_2tt (Figure 6) is only 3 wt. %). The EDX method and spectrophotometric measurements revealed considerably higher loading of Pt on TiO_2tt, 18 wt. %. There is agglomeration of TiO_2 upon introduction of sulfuric acid into Pt colloidal dispersion/TiO_2tt dispersion mixture (Figure 4b). Consequently, the
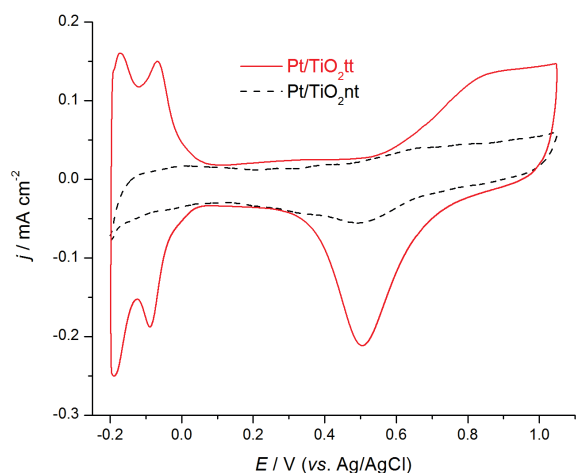
Figure 6. Cyclic voltammograms of Pt supported on thermally treated (Pt/TiO$_2$tt) and untreated (Pt/TiO$_2$nt) TiO$_2$ in de-aerated 0.1 M HClO$_4$, sweep rate 50 mV s^{-1}.

possibility for Pt particles to be trapped inside TiO$_2$ agglomerates, *i.e.*, within tightly joined 100 nm-sized TiO$_2$ particles (Figure 1c) is indicated.

CONCLUSIONS

Platinum nanoparticles, synthesized by a typical polyol procedure, were applied to prepare a composite material with TiO$_2$ of defined structure to be used as a potential catalytic material. The correlations between physicochemical properties of TiO$_2$ and the component distribution in the composite, and consequently its basic voltammetric response, were investigated.

Thermally treated (tt) and untreated (nt) TiO$_2$ powders, synthesized by forced hydrolysis of Ti chloride, consisted of 20-nm-sized particles joined into 200 nm-sized spherical clusters that formed μm-sized agglomerates. TiO$_2$nt was found to be mainly amorphous with only an indication of crystallization to anatase form, while the thermal treatment generated well-resolved, dominantly rutile structure of TiO$_2$tt.

An aqueous suspension of TiO$_2$ appeared to be stabilized upon addition of ethane-1,2-diol, present in the Pt dispersion with which the TiO$_2$ suspension was mixed to obtain 20 wt. % Pt loading in Pt/TiO$_2$tt.

While the voltammetric properties of Pt/TiO$_2$nt did not indicate clearly the Pt incorporation, the Pt loading in Pt/TiO$_2$tt was found to be around 18 wt. %. A basic check of the properties by cyclic voltammetry in acid solution showed that only 3 wt. % of Pt responded electrochemically. This result implies that Pt particles could be trapped inside TiO$_2$ agglomerates, and hence, do not contribute to the voltammetric response.

It is shown that Pt and TiO$_2$ could be easily combined into a composite catalyst, whereas further modifications of the synthesis toward more ordered composite structures are required to gain a real Pt/TiO$_2$ catalytic effect.

REFERENCES

[1] A. Fujishima, X. Zhang, D. A. Tryk, *Surf. Sci. Rep.* **2008**, *63*, 515.

[2] V. V. Panić, S. I. Stevanović, V. B. Mišković-Stanković, B. Ž. Jovanović, B. Ž. Nikolić, *J. Serb. Chem. Soc.* **2008** *73* 1211.

[3] J. M. Coronado, M. D. Hernández-Alonso in *Design of Advanced Photocatalytic Materials for Energy and Environmental Applications* (Eds.: J. Coronado, F. Fresno, M. D. Hernández-Alonso, R. Portela), Springer, Berlin, **2013**, pp. 85–101.

[4] V. V. Panić, B. Ž. Nikolić, *J. Serb. Chem. Soc.* **2008**, *73*, 1083.

[5] S. Sharma, B. G. Pollet, *J. Power Sources* **2012**, *208*, 96.

[6] A. Sclafani, J. M. Herrmann, *J. Phys. Chem.* **1996**, *100*, 13655.

[7] S. G. Neophytides, S. Zafeiratos, G. D. Papakonstantinou, J. M. Jaksic, F. E. Paloukis, M. M. Jaksic, *Int. J. Hydrogen Energy* **2005**, *30*, 393.

[8] P. P. Edwards, V. L. Kuznetsov, W. I. F. David, N. P. Brandon, *Energy Policy* **2008**, *36,* 4356.

[9] B. Sørensen, *Hydrogen and Fuel Cells, Emerging technologies and applications*, 2nd ed., Academic Press, Oxford, 2012, pp. 1–4

[10] S. Shafiee, E. Topal, *Energy Policy* **2009**, *37*, 181.

[11] R. Borup, J. Meyers, B. Pivovar, Y. S. Kim, R. Mukundan, N. Garland, D. Myers, M. Wilson, F. Garzon, D. Wood, P. Zelenay, K. More, K. Stroh, T. Zawodzinski, J. Boncella, J. E. McGrath, M. Inaba, K. Miyatake, M. Hori, K. Ota, Z. Ogumi, S. Miyata, A. Nishikata, Z. Siroma, Y. Uchimoto, K. Yasuda, K. Kimijima, N. Iwashita, *Chem. Rev.* **2007**, *107*, 3904.

[12] H. R. Colon-Mercado, B. N. Popov, *J. Power Sources* **2006**, *155*, 253.

[13] S. Hadži Jordanov, P. Paunović, O. Popovski, A. Dimitrov, D. Slavkov, *Bull. Chem. Technol. Macedonia* **2004**, *23*, 101.

[14]   J. C. Meier, C. Galeano, I. Katsounaros, J. Witte, H. J. Bongard, A. A. Topalov, C. Baldizzone, S. Mezzavilla, F. Schüth, K. J. J. Mayrhofer, *Beilstein J. Nanotechnol.* **2014**, *5*, 44.

[15]   A. Pozio, M. De Francesco, A. Cemmi, F. Cardellini, L. Giorgi, *J. Power Sources* **2002**, *105*, 13.

[16]   T. Tesfu-Zeru, M. Sakthivel, J.-F. Drillet, *Appl. Catal. B* **2017**, *204*, 173.

[17]   A. Marcu, G. Toth, P. Pietrasz, J. Waldecker, *C. R. Chim.* **2014**, *17*, 752.

[18]   M. Chena, M. Wanga, Z. Yanga, X. Wanga, *Appl. Surf. Sci.* **2017**, *406*, 69.

[19]   J. Xu, M. Zhao, S. Yamaura, T. Jin, N. Asao, *J. Appl. Electrochem.* **2016**, 46, 1109.

[20]   B. Li, D. C. Higgins, Q. Xiao, D. Yang, C. Zhng, M. Cai, Z. Chen, J. Ma, *Appl. Catal. B* **2015**, *162*, 133.

[21]   S. Bagheri, N. M. Julkapli, S. Bee, A. Hamid, *Sci. World J.* **2014**, *2014*.

[22]   G. R. Bamwenda, S. Tsubota, T. Nakamura, M.Haruta, *Catal. Lett.* **1997**, *44*, 83.

[23]   S. J. Tauster, S. C. Fung, R. T. K. Baker, J. A. Horsley, *Science* **1981**, *211*, 1121.

[24]   D. S. Kim, E. F. A. Zeid, Y. T. Kim, *Electrochim. Acta* **2010**, *55*, 3628.

[25]   A. Lewera, L. Timpermen, A. Roguska, N. Alonso-Vante, *J. Phys. Chem. C* **2011**, *115*, 20153.

[26]   C. Su, B.-Y. Hong, C.-M. Tseng, *Catal. Today* **2004**, *96*, 119.

[27]   M. G. Košević, G. M. Šekularac, V. V. Panić, *J. Electrochem. Sci. Eng.* **2016**, *6*, 29.

[28]   S. Stevanović, D. Tripković, J. Rogan, K. Popović, J. Lović, A. Tripković, V. M. Jovanović, *J. Solid State Electrochem.* **2012**, *16*, 3147.

[29]   E. Matijević, M. Budnik, L. Meites, *J. Colloid Interface Sci.* **1977,** *61*, 302.

[30]   G. Šekularac, M. Košević, I. Drvenica, A. Dekanski, V. Panić, B. Nikolić, *J. Solid State Electrochem.* **2016**, *20*, 3115.

[31]   B. Erdem, R. A. Hunsicker, G. W. Simmons, E. D. Sudol, V. L. Dimonie, M. S. El-Aasser, *Langmuir* **2001**, *17*, 2664.

[32]   S. S. Mali, C. A. Betty, P. N. Bhosale, P. S. Patila, *ECS J. Solid State Sci. Technol*. **2012**, *1*, M15.

[33]   S. Zhuiykov, *Ionics* **2009**, *15*, 507.

[34]   Y. J. He, J. F. Peng, W. Chu, Y. Z. Li, D. G. Tong, *J. Mater. Chem. A* **2014**, *2*, 1721.

[35]   A. A. Ismail, L. Robben, D. W. Bahnemann, *ChemPhysChem* **2011**, *12*, 982.